Compact Models for Squeeze−Film Damping in the Slip Flow Regime

Robert Sattler and Gerhard Wachutka

Institute for Physics of Electrotechnology,
Munich University of Technology
Arcisstr. 21, 80290 Munich, Germany; sattler@tep.ei.tum.de

ABSTRACT

We propose a mixed−level simulation scheme for squeeze film damping effects in microdevices, which makes it possible to include damping effects in system−level models of entire microsystems in a natural, physically−based and flexible way. Our approach allows also for complex geometries, large deflection and coupling to other energy domains. In this work, we focus on the extension of our model to the slip flow regime. To this end, the flow problem is separated into appropriate blocks. For each block the slip factor is derived analytically or extracted from FEM simulations based on the Navier−Stokes equation with slip boundary conditions. Our fully parametrized and, therefore, predictive mixed−level model could be verified by FEM and experimental analysis.

Keywords: squeeze−film damping, mixed−level modeling, compact model, slip flow, finite network.

1 INTRODUCTION

Movable structural parts in MEMS devices without expensive vacuum packaging are strongly affected by air damping. It is therefore that squeeze−film damping effects are an inherent part of the design and, hence, have to be taken into account to allow a predictive simulation of the transient behavior. However, it is prohibitive to use a continuous field solver for devices of real−world complexity. Instead, we follow a mixed−level approach, which makes it possible to reduce the model complexity by incorporating damping [1] and electrostatic [2] effects in system−level models in a physically correct and accurate manner. The damping model is based on the Reynolds equation, a simplified version of the Navier−Stokes equation (NSE), which is solved using the Finite Network method. The basic idea of our approach has been presented in [3]. In the terminology of Kirchhoffian Network variables, we consider the fluidic mass flow as generalized flux (”through”” variable), which is driven by the gradient of pressure acting as generalized force (”across” variable). Physically−based, scalable compact models are integrated in the network to correct for finite size effects and perforations in the structure (Fig.1).

All these compact models have recently been enhanced and validated. They are now thoroughly parametrized and can be rigorously derived from the Stokes equation [4].

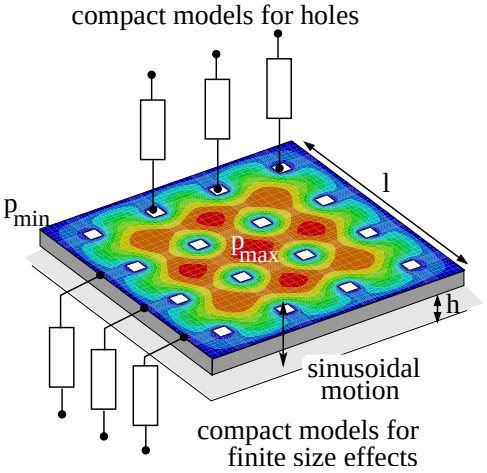

Fig 1: Elementary test structure: The colors indicate the pressure distribution below the actuating plate [3].

With this approach, we are able to perform predictive simulations of squeeze−film damping forces, which include physical parameters only and needs no longer the adjustment of fit parameters. Fig. 2 gives a more detailed view of the compact models and their connectivity with the Finite Network.

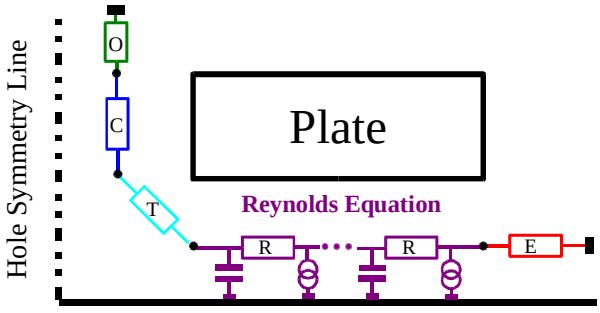

Fig 2: Schematic view of the mixed−level damping model. The Finite Network solves the nonlinear Reynolds equation for arbitrary geometry of the plate. The compact models account for corrections at the edge (E) and at perforations. The latter incorporates orifice flow (O), channel flow (C) and the transit flow (T) between the plate and the hole

2 RAREFACTION

With progressive miniaturization (e.g. the air gap underneath our demonstrator in Fig. 7 is only 1 µm), the effect of rarefaction has to be taken into account. Macroscopic fluids can be described by the NSE and the so−called "no−slip" boundary condition at the fluid−solid interface. As no discontinuities are allowed at the fluid−solid interface, the fluid velocity must be zero relative to the surface. But this boundary condition is only valid in thermodynamic equilibrium. In dilute gases the collision frequency between the fluid and the solid surface is not high enough to ensure equilibrium. Therefore a tangential velocity slip must be admitted:

$$u_{gas} - u_{wall} = \frac{2-\alpha}{\alpha} \cdot \lambda \frac{\partial u}{\partial n} \qquad (1)$$

This simple first−order slip model relates the slip velocity at the wall to the mean free path of the gas λ and the gradient of the gas velocity in the normal direction of the wall [5]. The tangential−momentum−accommodation coefficient α is defined as the fraction of molecules which are diffusively reflected. This coefficient has been introduced by Maxwell and depends on the gas, the solid and the surface finish and has to be determined experimentally. It lies typically between 0.2 and 0.8, where the upper limit is attained for most practical surfaces. For quantifying the degree of rarefaction, the Knudsen number Kn=λ/$\mathscr{L}$ is used, where $\mathscr{L}$ is a characteristic length of the flow (e.g. the diameter of a fluidic channel). If the Knudsen number exceeds the order of magnitude of 10^{-1}, the continuity assumption breaks down and the Boltzmann transport equation has to be used to describe the flow.

Kn<0.01	***0.01<Kn<0.1***	***0.1<Kn<10***	***Kn>10***
Continuum Flow	Slip Flow	Transit Flow	Free Molecular Flow

Tab. 1: Empirical classification of Knudsen number regimes

3 COMPACT MODELS

In the following we investigate the reduction of the fluidic resistance of each compact model due to slip flow.

3.1 Channel Flow

The compact models R and C in Fig. 2 are based on a Poiseuille channel flow. Under the constraints of a one dimensional channel flow the incompressible NSE reduces to: $\eta\, d^2 u_x / dn^2 = dp/dx$
(viscosity η , pressure p, flow direction x, velocity u).

Solving this equation with the slip boundary condition (eq. 1) results in eq. 2 for the fluidic resistance of a channel of length L and height h. If we transform this equation to cylindrical coordinates, we find the fluidic resistance for a circular tube with radius r (eq. 3).

$$R_{Channel} = \frac{\Delta p}{\rho \cdot v \cdot h} = 12 \frac{\eta}{\rho} \frac{L}{h^3} \cdot (1 + 6\,Kn)^{-1} \qquad (2)$$

$$R_{Tube} = \frac{\Delta p}{\rho \cdot v \cdot \pi r^2} = \frac{8}{\pi} \frac{\eta}{\rho} \frac{L}{r^4} \cdot (1 + 8\,Kn)^{-1} \qquad (3)$$

The last term in brackets gives the correction of the compact models due to slip flow. This slip factor is equals one for continuous flow (Kn=0). The fluidic resistance in the Reynolds equation (R, Fig. 2) is represented by eq. 2, as firstly derived by Burgdorfer [6]. The fluidic resistance for a circular tube (C, Fig. 2) is represented by eq. 3. This slip factor has also be named "effective viscosity" η_{eff} [10].

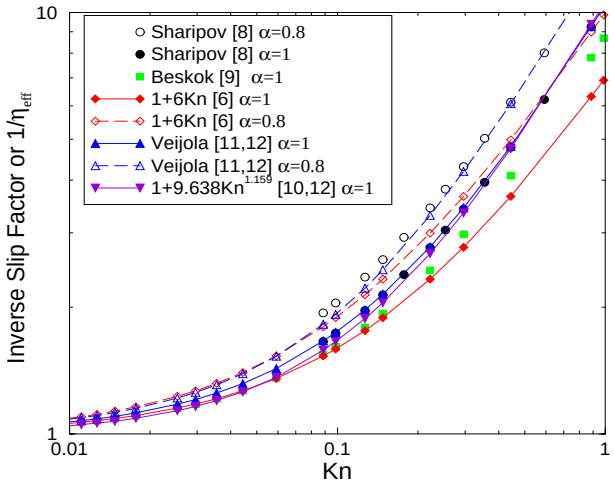

Fig. 3: Inverse slip factor for channel flow as calculated from various authors from atomistic simulations.

Fig. 3 illustrates that, with increasing Knudsen number, there is an increasing discrepancy between the simple slip model and the solution of the Boltzmann equation as reported by various authors. We used the simple model, on the one hand because of the uncertainties in the atomistic simulations, on the other hand because for intermediate Knudsen numbers the proper choice of the accommodation coefficient has much more impact than a higher order slip model. Hence, in the following diffusive reflection (α=1) is assumed.

3.2 Orifice Flow

The compact models E and O (Fig. 2) are based on viscous orifice flow, which can be derived from the Stokes equation. The velocity distribution in an elliptic orifice with the semi−axes a and b, the perimeter s and the area A is given by eq.4 [7]:

$$u(x,y) = \frac{A \cdot \Delta p}{\pi s \eta} \cdot \sqrt{1 - \frac{x^2}{a^2} - \frac{y^2}{b^2}} \qquad (4)$$

$$\dot{m} = \rho \iint_A u(x,y)\, dA \qquad (5)$$

Applying a slip velocity boundary condition and calculating the mass flow from eq. 5, we derived the fluidic resistance for two special cases of an elliptic orifice: A circular orifice of radius r (eq. 6) and a narrow slit of width h and length L with h << L (eq. 7).

$$R_{circular} = \frac{\Delta p}{\dot{m}} = \frac{3}{r^3}\frac{\eta}{\rho}[(1+2\,Kn)^{3/2}-(2Kn)^{3/2}]^{-1} \quad (6)$$

$$R_{slit} = \frac{16}{L\cdot h^2}\frac{\eta}{\rho}[\sqrt{2Kn}+(1+2Kn)\arcsin(1+2Kn)^{-1/2}]^{-1} \quad (7)$$

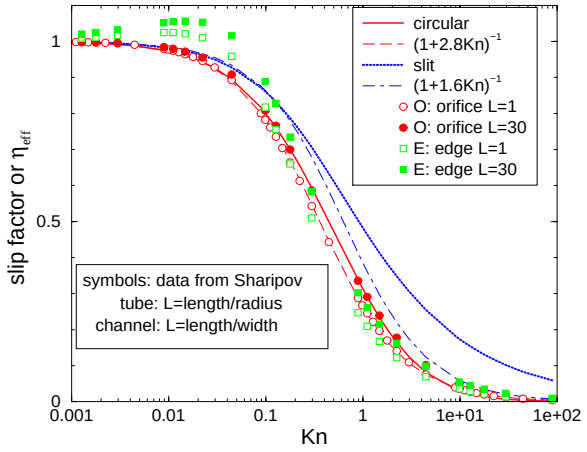

Fig. 4: Slip factor for the orifice calculated from eq. 5, 6 in comparison with data from Sharipov [8].

Sharipov solved the Boltzmann equation for channel flow and for tube flow of finite length. He describes the pressure drop at the orifice by an extra length of the channel. His tabulated results [8] have been converted into a slip factor for the orifice flow and are depicted together with our results in Fig. 4.

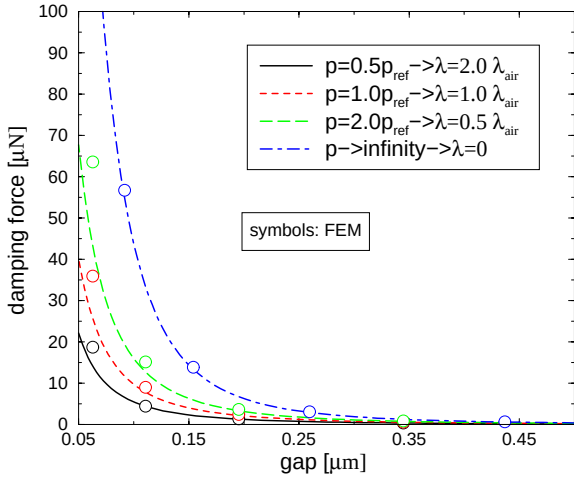

Fig. 5: Damping force on a disc (R=50 μm) moving with constant velocity towards ground in dependance of the mean free path.

In order to validate the slip factors for our compact models the slip flow boundary condition (eq. 1) was implemented in the NSE−solver of ANSYS. The computational expense of the FEM simulations was reduced by choosing a circular disc as our theoretical demonstrator. The Knudsen number depends on the mean free path which is inverse proportional to the ambient pressure. Fig. 5 demonstrates the influence of the ambient pressure on the damping force of the disc. Our mixed−level model agrees well with the solution of the NSE with slip flow boundary conditions. But for small gaps the Knudsen number increases and the slip factor $(1+6Kn)^{-1}$ underestimates the damping force on the disc. This is due to the moving boundary condition of the upper channel wall. All results in Fig. 3 are based on a channel with fixed walls, but this is usually not the case for a moving part of a MEMS device.

3.3 Transit Flow

So far only elementary structures such as tubes and channels have been investigated by numerical atomistic simulation. Therefore the slip factor for the transit resistances T in Fig. 2 cannot be found in literature. For this region it is difficult to define a Knudsen number, because the characteristic length scale $\mathscr{L}$ could be the diameter of the hole (2r in eq. 3) or the gap under the plate (h in eq. 2). In Fig. 6 the latter was chosen. The slip factor (eq. 8) in the compact model for the transit resistance (T) has been adjusted with reference to the FEM simulation of the NSE with slip boundary conditions (eq. 1). Figure 6 also illustrates that our mixed−level model can reproduce the damping force on a punched disc for various hole sizes.

$$\frac{R_{Transit}^{Slip}}{R_{Transit}^{no\ Slip}} = (1+1\,Kn)^{-1} \quad (8)$$

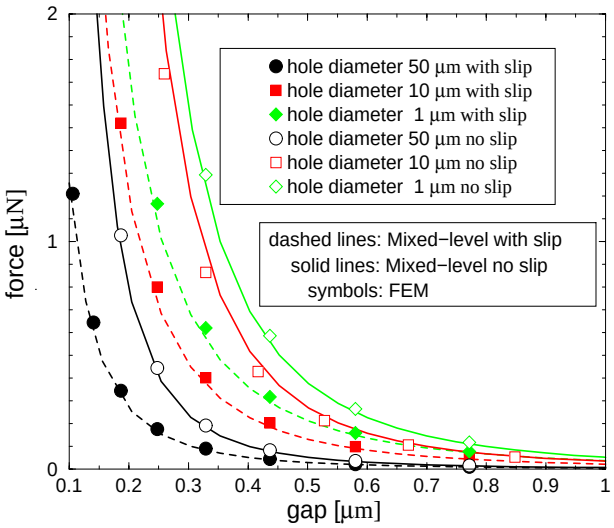

Fig. 6: Damping force acting on a punched disc which moves with constant velocity towards ground (R=50 μm).

4 EXPERIMENTAL DEMONSTRATOR

Finally, we compare our mixed−level model with experimental data extracted from measurements on industrial prototypes of the microrelay shown in Fig. 7:

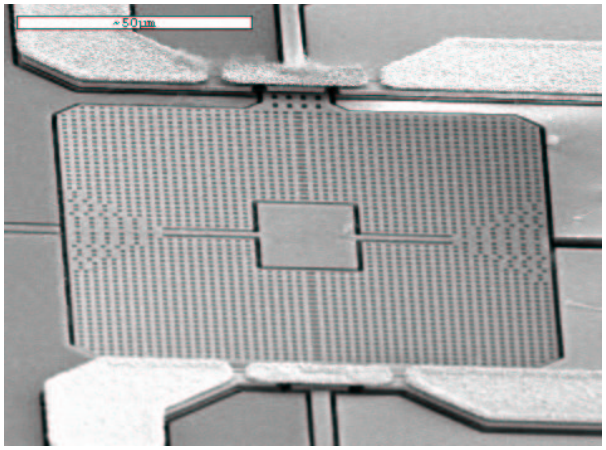

Fig. 7: SEM image of an electrostatic microswitch perforated with about 3000 etch holes.

The plate of the torsional switch is highly perforated with small etch holes. Three different types of perforations have been fabricated. They differ in the ratio of the hole area to the total cell area. Fig. 8 shows the influence of slip flow on the fluidic resistance of a single cell. With and without slip flow the mixed−level model agrees well with the FEM simulation of the NSE.

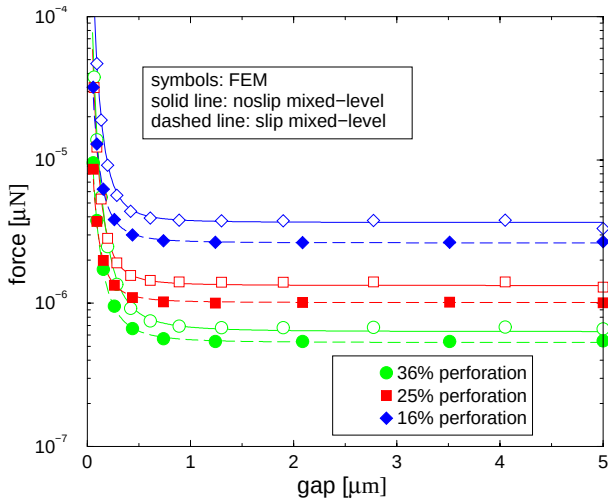

Fig. 8: Damping force on a single cell of the microswitch in Fig. 7 moving with constant velocity towards ground.

Fig. 9 shows the off−to−on and on−to−off switching transients of the same three device variants. The simulation transients are in excellent agreement with the measured characteristics, which demonstrates the high quality and predictive capability of our modeling approach.

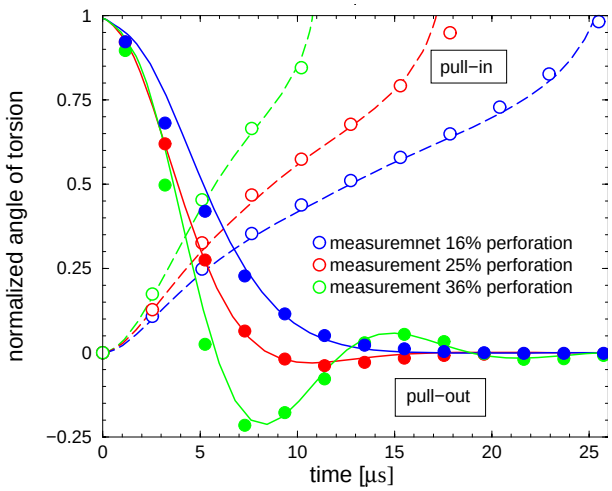

Fig. 9: Measurement of the pull−in and pull−out behavior of the microswitch in comparison with our mixed−level model.

CONCLUSION

We demonstrated that our mixed−level model based on a physical device description in terms of a standard hardware description language (VHDL−AMS) can successfully be extended to the slip flow regime. For every elementary structural part of the plate (Fig. 2) the proper model has to be chosen. Therefore it is misleading to use the term “effective viscosity”, as this suggests using one single formula everywhere. All slip flow models in conjunction with Reynolds equation presented so far (Fig. 3) are based on the channel flow with fixed walls. But for real devices at least one wall is movable. With increasing degree of rarefaction the correct choice of the boundary conditions gain importance. Therefore atomistic simulations have to be done that take care of this effect.

REFERENCES

[1] R. Sattler, G. Schrag, G. Wachutka, MSM’02, pp. 124−127.
[2] R. Sattler, G. Schrag, G. Wachutka, MSM’03, pp. 284−287.
[3] G. Schrag, G. Wachutka, Sensors and Actuators A 97−98 (2002), pp. 193 200.
[4] R. Sattler, G. Wachutka, *Improved Physically−Based Mixed−Level Damping Model*, submitted to DTIP’04, Montreux, Switzerland.
[5] S.A. Schaaf, F.S. Sherman, *“Skin Friction in Slip Flow”*, Journal of Aeronautical Sciences, vol. 21, no. 2, 1953,pp. 85−90.
[6] A. Burgdorfer, “ASME Journal of Basic Engineering, March 1959, pp. 94−100.
[7] H. Hasimoto, J. Phys.Soc.Japan, 13, no 5,1958, pp. 633−639.
[8] F. Sharipov, V. Seleznev, *Data on Internal Rarefied Gas Flow*, J.Phys.Chem.Ref.Data,Vol.27, No.3, pp.657−706, 1998.
[9] P. Bahukudumbim A. Beskok, *A Phenomenological Lubrication Model for the Entire Knudsen Regime*, J. Micromech. Microeng. 13, No. 6, November 2003, pp.873−884.
[10] Veijola,..,Sensors and Actuators A 48 (1995), pp. 239−248.
[11] Veijola,..,Sensors and Actuators A 66 (1998), pp. 83−92.
[12] Fukui,Kaneko, J.Tribol.Trans.ASME, 112(1990), pp.78−83.